

Hiromu Sakurai¹, Yoshiko Murashima¹, Yuji Fujitani², and Nobuyuki Takegawa³

¹National Institute of Advanced Industrial Science and Technology (AIST) ²National Institute for Environmental Studies (NIES) ³Tokyo Metropolitan University

Contact: hiromu.sakurai@aist.go.jp

Introduction

In our recent field studies of nanoparticles emitted from aircrafts at an airport (Fushimi et al., 2019), we observed a strong peak at about 10 nm when aircraft exhaust plumes hit the measurement site near a runway in size distribution measurements made at a rate of 1 Hz with a TSI Engine Exhaust Particle Sizer (EEPS) spectrometer model 3090 (**Figure 1**).

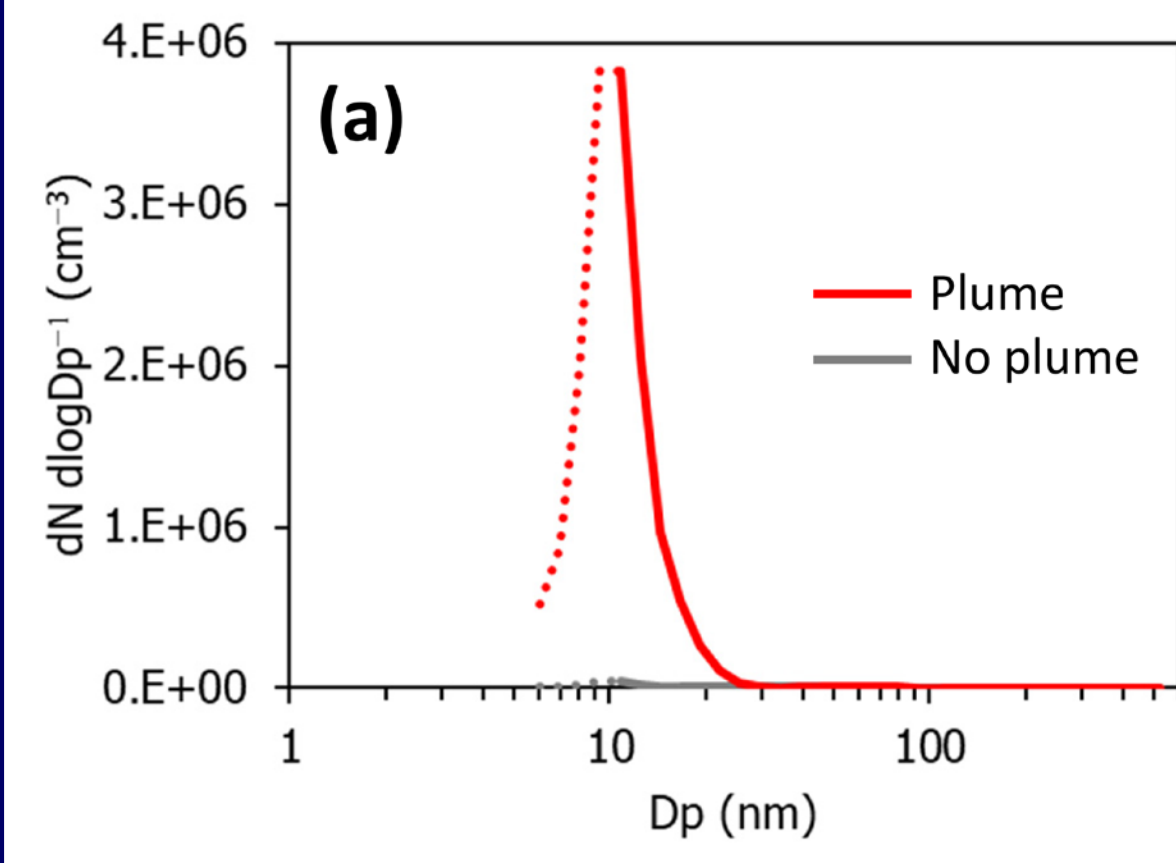


Figure 1. Particle number size distributions with (red) and without (grey) aircraft exhaust plumes. This figure is a reproduction of Figure 3(a) in: Fushimi A., Saitoh K., Fujitani Y., Takegawa N. (2019). Identification of jet lubrication oil as a major component of aircraft exhaust nanoparticles, *Atmos. Chem. Phys.*, 19, 6389–6399.

We were not confident about the accuracy of the size distribution around 10 nm that was obtained with the EEPS. *Was the mode size really 10 nm? Or, did the size distribution appear so because the detection efficiency of the EEPS sharply dropped below 10 nm while the actual size distribution did not have a peak at 10 nm?* To answer these questions, we investigated the accuracy of y-axis, i.e., particle size distribution and number concentration, measured by the EEPS in the size range from 6 nm to 200 nm, with particular attention at about 10 nm.

Experimental methods

The EEPS, a reference condensation particle counter (Ref. CPC), and a reference scanning mobility particle sizer (Ref. SMPS) sampled test aerosol particles from the same source and measured concentration and/or size distribution simultaneously (**Figure 2**).

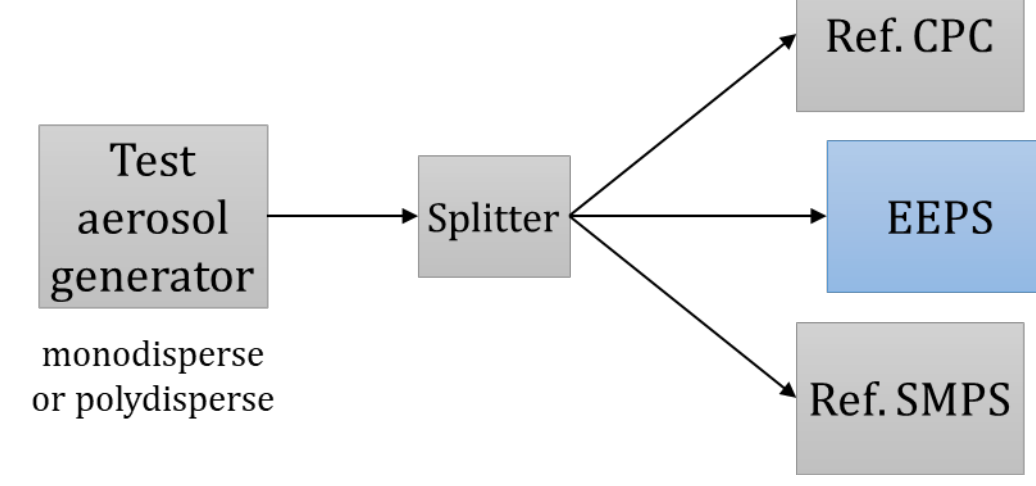


Figure 2. Experimental setup. Ref. CPC was either TSI 3771 (30 – 200 nm) or 3775 CPC (< 20 nm). Ref. SMPS was a TSI nano (3085) DMA with TSI 3082 platform/3088 soft x-ray/3775 CPC, without impactor, and with both DLC and MCC on AIM 10.2.

The following two tests were made for the EEPS:

1. about the total concentration (C) of DMA-classified monodisperse particles against Ref. CPC in the size range from 30 to 200 nm. For the EEPS, the total concentration was calculated by integrating size distribution for the peak;
2. about the size distribution density function ($dC/d\log d$) of polydisperse particles against Ref. SMPS for each size bin at sizes about 10 nm. The SMPS size bin resolution was set at 16 bins per decade, which was equal to that of the EEPS.

Both Ref. CPC and Ref. SMPS were calibrated against AIST's number concentration standard. In the EEPS, the *default* instrument matrix was used.

Tests in the 30 – 200 nm range with monodisperse particles

Polystyrene latex (PSL) spheres were used as monodisperse test particles at 30, 60, 100 and 200 nm to investigate the accuracy of the measured concentration.

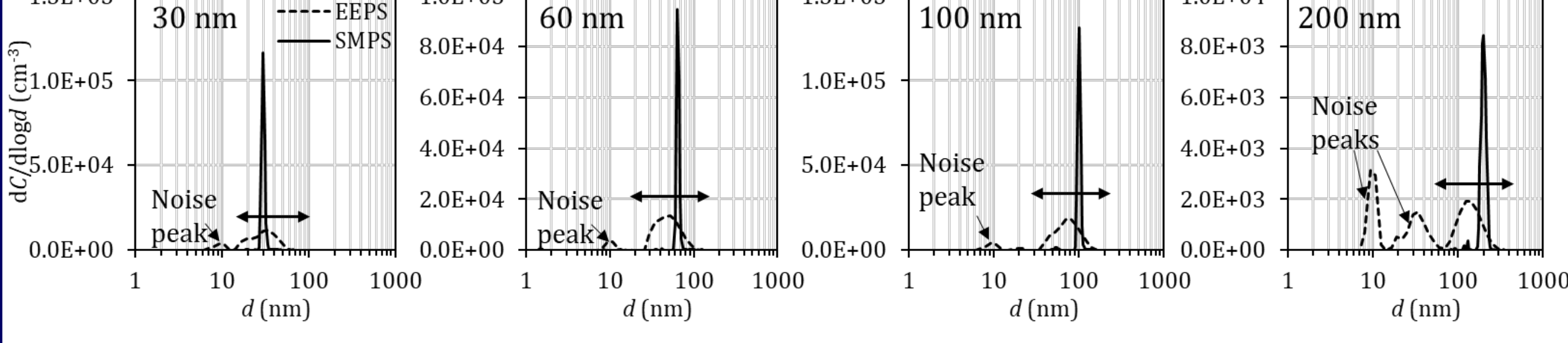


Figure 3. Size distribution spectra by the EEPS and Ref. SMPS of the four PSL particles.

As reported in the literature, the size distributions by the EEPS were broader than those by Ref. SMPS for the monodisperse particles. Underestimation of particle size was observed at 60, 100, and 200 nm (**Figure 3**).

There were noise peaks at about 10 and 30 nm in the EEPS spectra, which could not have been eliminated by zeroing. They were excluded from the integration when possible. The double-sided arrows indicate the integrated ranges.

Figure 4 summarizes the comparison of the total concentration between the EEPS (C_{EEPS}) and Ref. CPC (C_{ref}^*).

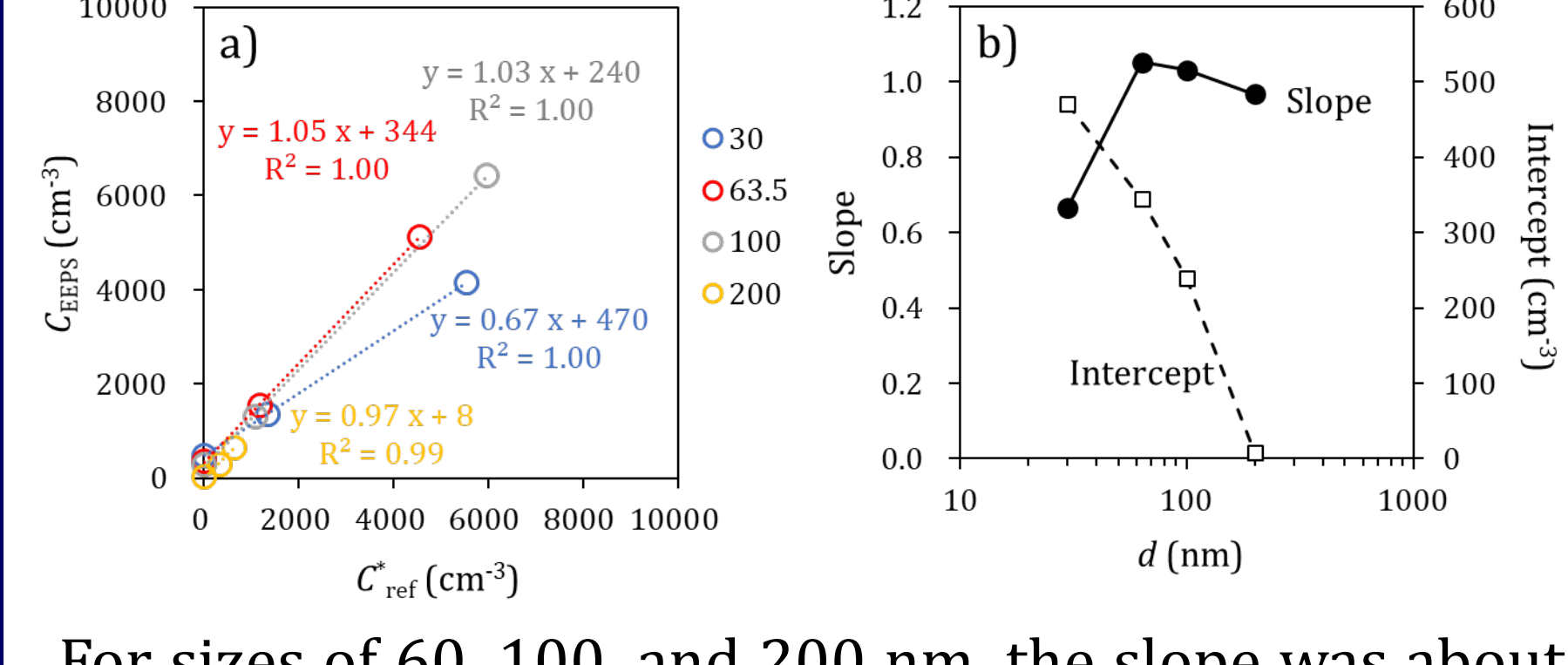


Figure 4. a) A scattering plot for the total concentration by the EEPS and that by Ref. CPC for the four particle sizes. b) the slope and intercept obtained by linear regression of the data in a) for each size.

For sizes of 60, 100, and 200 nm, the slope was about unity, which indicates that the total concentration by EEPS was accurate. At 30 nm, the slope was 0.67, which indicates that EEPS underestimated by 40 %. There were some non-zero signal at 30, 60, and 100 nm which was indicated as the intercept of 10^2 – 10^3 cm $^{-3}$.

Tests at about 10 nm with polydisperse particles

Polydisperse sintered silver particles (i.e., without DMA classification) with the mode diameter of 6, 8, and 10 nm were used as test particles to investigate the accuracy of the size distribution density function ($dC/d\log d$) in the range from 6 to 20 nm. Comparisons were made against Ref. SMPS (**Figure 5**).

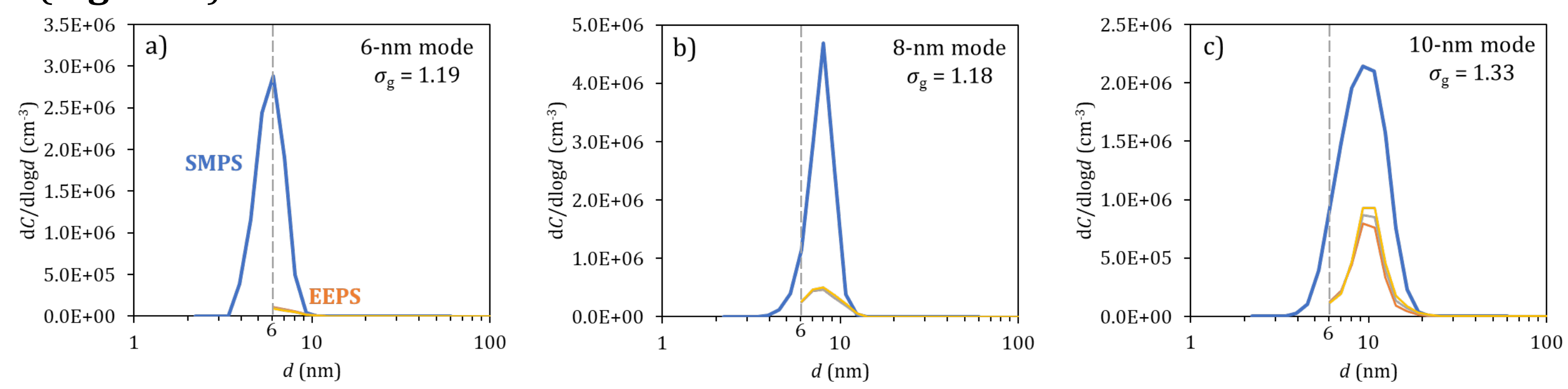


Figure 5. Size distribution spectra of the EEPS and Ref. SMPS for polydisperse silver particles of (a) 6-nm, (b) 8-nm, and (c) 10-nm mode diameters.

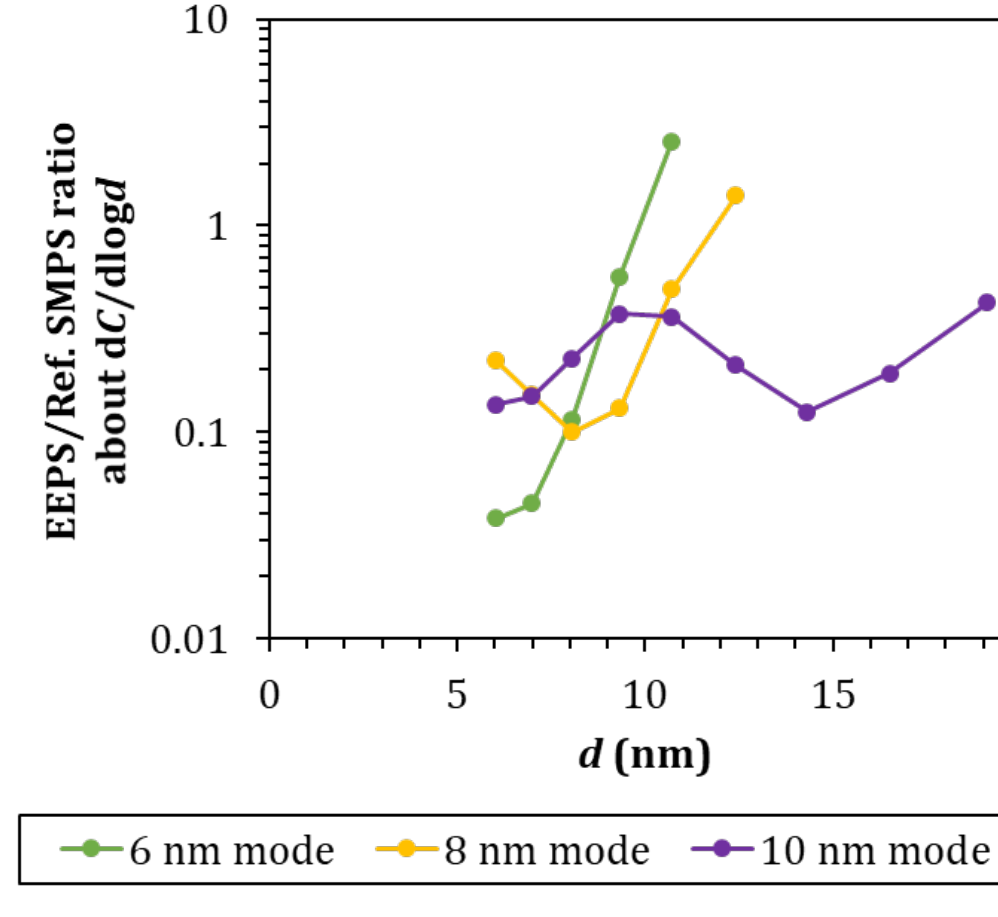


Figure 6

While the EEPS significantly underestimated the concentration, the shape of the size distribution by the EEPS was similar to that of Ref. SMPS. This implies that the observation of the 10-nm peak for aircraft exhaust in Fushimi et al. (2019) was real. The EEPS/Ref. SMPS ratios of $dC/d\log d$ were different among the three spectra. **Figure 6** shows the ratio in logarithmic scale at all (non-zero) size bins for the three size distributions in Figure 5. The ratio varied by nearly an order of magnitude at some of the size bins. This implies that, in contrast to the SMPS, an application of a simple correction factor to each size bin cannot improve the accuracy of $dC/d\log d$ of the EEPS.

Deriving more accurate $dC/d\log d$ by EEPS using raw current data

We looked into a possibility to improve the accuracy of EEPS size distribution functions by using the raw current data for the 22 electrode channels in the output files. Since unipolarly-charged particles occupy only a limited number of charge states in the size range about 10 nm, we speculated that a simple data inversion algorithm for reducing $dC/d\log d$ from raw current data may give rather accurate results.

First, it was assumed that the current signal of an electrode channel should correlate well with $dC/d\log d$ of one of the size bins of Ref. SMPS. Using the data in Figure 5, for each electrode channel, correlations of the EEPS current with the $dC/d\log d$ values of Ref. SMPS for several size bins were compared, and the combination of the best correlation was identified. **Figure 7** shows an example for the comparison for the electrode channel #2. The size bin of 8.06 nm showed the best correlation for #2.

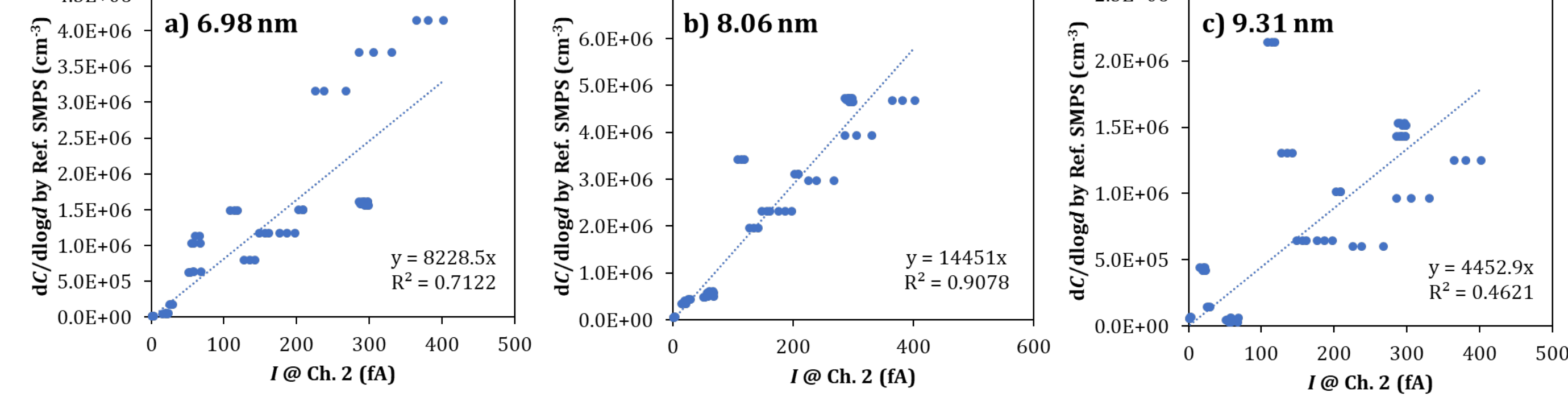


Figure 7. Correlation plots between the EEPS current of the electrode channel #2 and $dC/d\log d$ by Ref. SMPS at a) 6.98 nm, b) 8.06 nm, and c) 9.31 nm.

Table 1 shows the best combinations of the EEPS electrode channel and the size bin of Ref. SMPS.

Table 1

Electrode channel #	SMPS size bin d (nm)	Sensitivity Coeff. (cm 3 fA $^{-1}$)	R^2
1	6.98	5.43×10^4	0.938
2	8.06	1.45×10^4	0.908
3	9.31	7.46×10^3	0.815
4	10.7	2.15×10^3	0.963
5	14.3	1.12×10^3	0.915
6	19.1	7.37×10^2	0.984

Second, the sensitivity coefficients in Table 1 were applied to the raw EEPS current data for the measurements in Figure 5 to calculate $dC/d\log d$. The obtained $dC/d\log d$ are plotted in **Figure 8** with $dC/d\log d$ of Ref. SMPS. The agreement of $dC/d\log d$ between the EEPS and Ref. SMPS improved dramatically. The agreement was similarly good for the three size distributions.

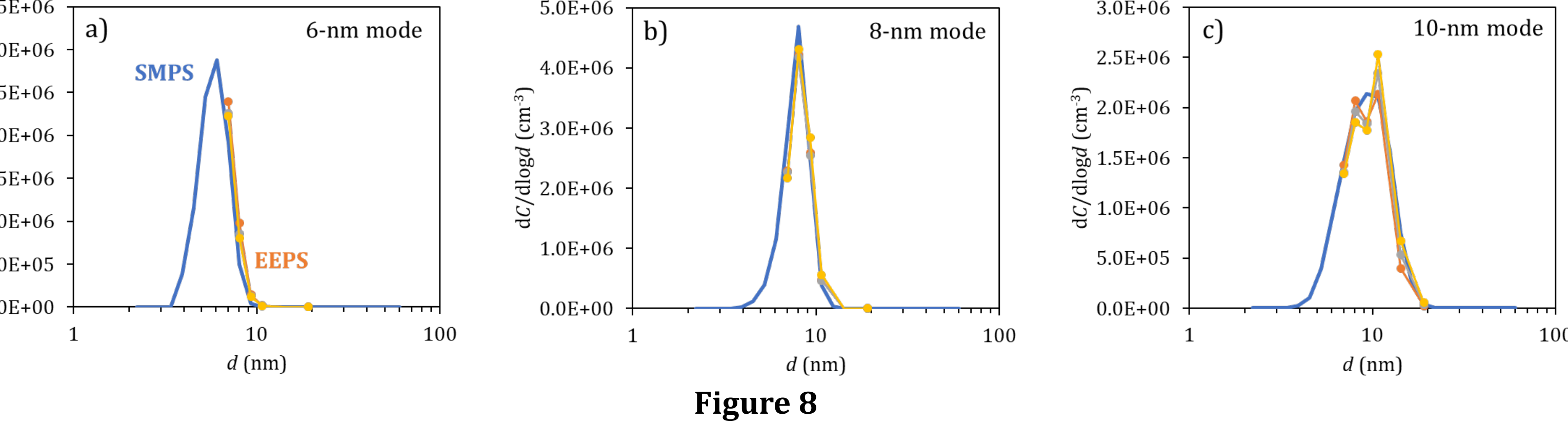


Figure 8

The improved agreement with Ref. SMPS indicates that the simple inversion algorithm used in this study worked well in the size range from 6 to 20 nm for these size distributions in which sub-20 nm particles dominated.

Better, more robust sensitivity coefficients could be obtained by adding more data points with different test particles to the regression analysis in Figure 7. The validity of this inversion algorithm will be further investigated in our future study.